

## THE NATURE OF THE HARD-X-RAY EMITTING SYMBIOTIC STAR RT CRU

G. J. M. LUNA

Instituto de Astronomia, Geofísica e Ciências Atmosféricas, Universidade de São Paulo, Rua do Matão 1226, Cid. Universitaria, São Paulo, Brazil 05508-900

AND

J. L. SOKOLOSKI

Columbia Astrophysics Lab. 550 W120th St., 1027 Pupin Hall, Columbia University, New York, New York 10027, USA

*Draft version October 27, 2018*

### ABSTRACT

We describe *Chandra* High-Energy Transmission Grating Spectrometer observations of RT Cru, the first of a new sub-class of symbiotic stars that appear to contain white dwarfs (WDs) capable of producing hard X-ray emission out to greater than 50 keV. The production of such hard X-ray emission from the objects in this sub-class (which also includes CD –57 3057, T CrB, and CH Cyg) challenges our understanding of accreting WDs. We find that the 0.3 – 8.0 keV X-ray spectrum of RT Cru emanates from an isobaric cooling flow, as in the optically thin accretion-disk boundary layers of some dwarf novae. The parameters of the spectral fit confirm that the compact accretor is a WD, and they are consistent with the WD being massive. We detect rapid, stochastic variability from the X-ray emission below 4 keV. The combination of flickering variability and a cooling-flow spectrum indicates that RT Cru is likely powered by accretion through a disk. Whereas the cataclysmic variable stars with the hardest X-ray emission are typically magnetic accretors with X-ray flux modulated at the WD spin period, we find that the X-ray emission from RT Cru is not pulsed. RT Cru therefore shows no evidence for magnetically channeled accretion, consistent with our interpretation that the *Chandra* spectrum arises from an accretion-disk boundary layer.

*Subject headings:* binary stars: general — white dwarf: accretion – X-rays

### 1. INTRODUCTION

Symbiotic stars are interacting binaries in which a hot, compact star accretes from the wind of a red-giant companion. Although a few symbiotics contain neutron-star accretors (e.g., GX 1+4, 4U 1700+24, 4U 1954+31, IGR J16194-2810; Davidsen et al. 1977; Masetti et al. 2002; Galloway et al. 2002; Masetti et al. 2007a,b), the accreting compact object is usually a white dwarf (WD). Typical binary separations are on the order of AU, with orbital periods on the order of a few hundred days to a few decades (Kenyon 1986; Belczyński et al. 2000). Symbiotics can thus be thought of as very large cousins of cataclysmic variables (CVs). The accretion rate onto the WD appears to be high enough in most symbiotic systems that accreted material is burned quasi-steadily in a shell on the WD surface, producing a high UV luminosity (Sokoloski et al. 2001; Orío et al. 2007). Although accretion disks are likely to exist around the WDs in some symbiotics (Livio 1997; Sokoloski & Kenyon 2003), there is little direct evidence for these disks. Finally, the red-giant wind produces a dense nebula that surrounds the system.

Most symbiotic stars with detectable X-ray emission display soft, or supersoft, thermal X-ray spectra. As in the supersoft X-ray sources, the lowest-energy X-rays could emanate directly from material burning quasi-steadily on the WD surface (Jordan et al. 1994; Orío et al. 2007). Based on a survey of symbiotics with *ROSAT*, Müerset et al. (1997) proposed that symbiotics be classified according to the hardness of their X-ray

spectra. They labeled sources with supersoft spectra  $\alpha$ -types, sources with the slightly harder spectra likely to arise from collision of the red-giant and white-dwarf winds  $\beta$ -types, and systems with the hardest spectra that might be indicative of neutron stars  $\gamma$ -types. Although more recent observations using the broader X-ray coverage and greater sensitivity of *Chandra* and *XMM-Newton* have shown that some symbiotics do not fit into the simple  $\alpha/\beta/\gamma$  classification scheme (e.g., Z And and *o* Ceti; Sokoloski et al. 2006; Karovska et al. 2005), most still appear to produce primarily soft X-rays ( $E < 3$  keV).

With the advent of the sensitive hard X-ray detectors on the *Swift* and INTEGRAL satellites, a new picture has emerged. Some symbiotic stars can produce X-ray emission out to greater than 50 keV. Such hard X-ray emission has so far been detected from 4 symbiotics thought to harbor WDs – RT Cru (Chernyakova et al. 2005; Bird et al. 2007), T CrB (Tueller et al. 2005; Luna et al. 2007), CH Cyg (Mukai et al. 2007) and CD - 57 3057 (Masetti et al. 2006; Bird et al. 2007). Although the origin of this hard X-ray emission is not known, there are some underlying similarities between these hard X-ray emitting symbiotics. Unlike most other symbiotic stars, they display a high incidence of optical flickering. They also tend to have low optical line strengths, indicating that they are often only “weakly” symbiotic. Both the visibility of the optical flickering (which in most symbiotics is overwhelmed by reprocessed shell-burning emission; Sokoloski 2003) and the weakness or low-ionization-state of the optical lines suggest that quasi-steady shell burning is not taking place in these objects, either because: 1) the WD is more massive, or 2) the accre-

tion rate is lower than in other symbiotics. Hard X-ray emission might therefore be a proxy for high WD mass. In fact, at least one of the hard-X-ray symbiotics, T CrB, is a recurrent nova and contains a high-mass WD (Hachisu & Kato 2001). Finally, jet production appears to be more common in flickering symbiotics, and one of the 4 hard X-ray symbiotics – CH Cyg – regularly produces jets (Taylor et al. 1986; Karovska et al. 1998; Crocker et al. 2001, 2002). Other WDs in hard X-ray symbiotics might thus also harbor jets.

Cieslinski et al. (1994) classified RT Cru as a symbiotic star based on its optical spectrum. They noted that the lack of strong high-ionization emission lines and the very weak forbidden emission lines make the optical spectrum similar to that of T CrB. They detected optical flickering in the U band with a time scale of a few tens of minutes. Except for GX 1+4 (Jablonski et al. 1997; Chakrabarty & Roche 1997), none of the neutron-star containing symbiotic stars produce optical flickering (e.g. Sokoloski et al. 2001), which is common in CVs, or show Balmer or He II emission lines (Masetti et al. 2007b). The presence of optical flickering and Balmer and He II emission lines from RT Cru (Cieslinski et al. 1994) suggests that it therefore contains an accreting WD rather than a neutron star. Reddening estimates from optical spectra and infrared magnitudes (coupled with the assumption that the radius of the M5 III red giant is about 0.5 AU; van Belle et al. 1999) suggest that RT Cru is between 1.5 and 2 kpc away (J. Miłojewska, *private communication*).

In 2003 and 2004, the IBIS instrument on board INTEGRAL detected hard X-ray emission extending out to  $\sim 100$  keV from the source IGR J12349-6434, which Chernyakova et al. (2005) found to have a 20-60 keV flux density of  $\sim 3$  mCrab. Masetti et al. (2005) suggested an association between IGR J12349-6434 and RT Cru, which observations with the *Swift* satellite later confirmed (Tueller et al. 2005). The long-term optical light curve from the AAVSO indicates that at the time of the INTEGRAL observations, RT Cru was in an optical bright state; it brightened from 13.5 to 11.5 mag sometime between 1998 and 2000. Between 2000 and 2005, the optical brightness slowly decreased to approximately 12.1 mag. The short (4.7 ks) *Swift* observation of 2005 August showed that between 2003 and 2005, the hard X-ray flux also decreased.

In this paper, we describe *Chandra* High Energy Transmission Grating (HETG) observations of RT Cru, the first member of a new class of hard X-ray emitting symbiotic WDs. We detail the observations and data reduction in §2 and the results from spectral and timing analyses in §3. In §4, we discuss our interpretation of the observations, which confirm that the accreting compact object in RT Cru is a WD and provide some of the most direct evidence to date for an accretion disk around a wind-fed WD in a symbiotic system. In this section, we also discuss the implications of a system that can accelerate particles to relativistic speeds and produce X-ray emission out to greater than 50 keV being powered by an accreting WD. We summarize our conclusions in §5.

## 2. OBSERVATIONS AND DATA REDUCTION

On 2005 October 19, the *Chandra* X-ray Observatory performed a 50.1 ks Director’s Discretionary Time obser-

vation of RT Cru using the HETG (Canizares et al. 2005) and the ACIS-S detector (ObsId 7186, start time 10:21:12 UT). We requested the DDT observation to attempt to catch RT Cru in the optical bright state that appeared to be associated with hard X-ray emission. We used the HETG instrument because the *Swift* XRT observation of 2005 August hinted at several possible emission-line complexes. The data were collected in Timed Exposure mode, in which the CCD chips were read out every 2.54 s. The data were telemetered back to earth in Faint mode, which conveys photon arrival times, event amplitudes, and additional information for evaluating the validity of each event. We reduced the data according to standard procedures using the software package CIAO 3.3<sup>1</sup>. We extracted a spectrum from the undispersed light (the zeroth-order spot, which fell on the S3, back-illuminated chip) using a circular extraction region with a radius of 6'' centered on the source coordinates:  $\alpha = 12^{\text{h}} 34^{\text{m}} 43.74^{\text{s}}$  and  $\delta = -64^{\circ} 33'56.0''$ . To obtain the background for the zeroth-order light, we extracted photons from a source-free circular region on the same CCD. We grouped the spectrum, which is shown in Fig. 1, to have at least 50 counts per bin. The average zeroth-order source count rate was  $0.11 \text{ c s}^{-1}$ .

For the dispersed light from both of the HETG sets of gratings – the Medium Energy Grating (MEG) and the High Energy Grating (HEG) – we extracted spectra from each of the  $m = \pm 1, \pm 2$ , and  $\pm 3$  orders individually (using the CIAO software tool *dmtype2split*). To obtain the background for the dispersed light, we extracted counts from rectangular regions on either side of the spectral image. The count rate in the HEG and MEG  $m \pm 1$  orders was  $0.042 \text{ c s}^{-1}$  and  $0.034 \text{ c s}^{-1}$ , respectively. Although the dispersed spectral orders contained too few counts to produce a high signal-to-noise-ratio spectrum of lines spanning the full energy range of the instrument, the combined  $m = \pm 1$  spectrum (grouped at twice the full width at half maximum of  $0.012\text{\AA}$ ) provided good-quality data in the region around the Fe  $K\alpha$  emission-line complex. We therefore used the the zeroth-order spectrum for continuum fitting and the dispersed ( $m = \pm 1$ ) spectra primarily for analysis of the Fe lines. The HEG and MEG  $m = \pm 2$  and  $\pm 3$  spectra helped confirm the Fe line identifications. For spectral fitting of both the zeroth and higher order photons, we used the standard software packages Xspec (Arnaud 1996) v12.3.0 and ISIS (Houck 2002). The background contributed less than 1% of the total extracted dispersed and undispersed light.

We generated light curves in the energy bands 0.3–4.0 keV and 4.0–8.0 keV by extracting counts (with CIAO) from a region containing the zeroth-order spot and the  $m = \pm 1$  dispersed orders of both the HEG and MEG. Since we estimated there to be only  $\sim 70$  background counts in this extraction region during the course of the observation (compared to more than 9000 source counts), we did not background-subtract the light curves.

At high count rates, two or more photons can arrive close enough together in time that they appear to be a single event. This “pileup” phenomenon can cause a spectrum to become distorted and the count rate to be reduced. To confirm that the zeroth order spectrum was

<sup>1</sup> Chandra Interactive Analysis of Observations (CIAO), <http://xc.harvard.edu/ciao/>.

not affected by pileup, we divided the number of counts at the peak of the point spread function of the undispersed light by the number of 2.54-s frames in the observation to obtain an upper limit on the number of counts per pixel per frame. The resulting 0.08 counts per pixel per frame is well below the 1 count per pixel per frame where pileup can become important (Harris et al. 2004). Moreover, the average count rate in the zeroth order was significantly less than one count per frame time, indicating that the light curve was not significantly distorted by the saturation that can occur at higher count rates (i.e., higher pileup fractions). The pileup fraction in the higher-order spectrum was negligible.

### 3. ANALYSIS AND RESULTS

#### 3.1. Spectral Analysis

To model the X-ray spectrum, we first consider simple, single-component continuum models. We fitted these models to the binned 0.3 – 8.0 keV zeroth-order spectrum (above 8.0 keV, the noise rises and the quantum efficiency drops sharply). Absorbed single-component emission models such as a thermal plasma, powerlaw, or blackbody (plus Gaussian lines) do not produce acceptable fits. Even if we include complex absorption, such as an absorber that only partially covers the source, a powerlaw distribution of absorbers (as seen in some magnetic CVs; e.g., Done & Magdziarz 1998), or a “warm” ionized absorber, single-component emission models still do not produce acceptable fits.

Including an additional broad-band emission component improves the fitting results. The spectrum is formally well fitted with a highly absorbed, optically thin thermal plasma (Mekal model in Xspec), plus a moderately absorbed non-thermal powerlaw component. Since there is some degeneracy between the amount of absorption and the powerlaw index, we determine the powerlaw index by fixing the plasma temperature,  $T$ , and fitting the spectrum above 4 keV, where absorption is relatively unimportant. The resulting photon index is  $\Gamma = 1.05_{0.78}^{1.29}$ , where  $\Gamma$  is given by  $dF_N/dE = K(E/E_0)^{-\Gamma}$ ,  $dF_N/dE$  is the photon flux density,  $E_0$  is 1 keV,  $K$  is the normalization constant, and the superscripts and subscripts are 90% confidence upper and lower limits, respectively. The photon index is not sensitive to the value to which we fix  $T$ . We determined the remaining model parameters by fixing  $\Gamma$  to 1.1 and letting the other parameters vary. The thermal plasma has  $kT = 8.6_{6.1}^{12.4}$  keV and an absorbing column  $n_H = 9.3_{7.2}^{12.5} \times 10^{23}$  cm $^{-2}$ . The powerlaw component has an absorbing column of  $n_H = 7.3_{6.3}^{8.7} \times 10^{22}$  cm $^{-2}$  and a normalization  $K = 1.2_{0.98}^{2.9} \times 10^{-3}$  photons cm $^{-2}$  s $^{-1}$  keV $^{-1}$ . To obtain an acceptable fit to the line emission, the model required abundances of about 0.3 times solar (using the abundances of Anders & Grevesse 1989). Because of the large column density absorbing the thermal emission in this model, the powerlaw component dominates below approximately 4 keV, and the thermal emission dominates above 4 keV. We also obtained a formally acceptable fit with a highly absorbed powerlaw and a moderately absorbed thermal plasma. In that case, the thermal plasma dominated the low-energy portion of the spectrum, and the powerlaw dominated the high-energy part of the spectrum.

Finally, we consider the isobaric cooling-flow model that has worked well for both magnetic and non-magnetic CVs. In this model (Mkcfw; Mushotzky & Szymkowiak 1988), gas is assumed to radiatively cool from a high post-shock temperature under conditions of constant pressure. Such an isobaric cooling flow has a differential emission-measure distribution that is a flat function of temperature. The gas is also assumed to be optically thin. This cooling flow model provides a good fit to the data. We find that the initial post-shock temperature is quite high. Although our 0.3–8.0 keV spectrum does not allow a high-confidence determination of this parameter, the formal 90% confidence lower limit for the initial temperature is  $kT_{max} = 55$  keV. The minimum cooling-flow temperature is consistent with the smallest value allowed by the Xspec Mkcfw model ( $kT_{min} = 80.8$  eV), indicating that the gas does indeed remain optically thin as it cools. Allowing the differential emission measure to have a powerlaw distribution (with the Cemkl model in Xspec) did not improve the fit. As with the two-component continuum model, the cooling-flow model requires significant absorption. The abundances may also be sub-solar (0.3 times solar, using the abundances of Anders & Grevesse 1989). The best absorption model consists of both a photoelectric absorber that fully covers the source and another that only partially covers it. Table 1 lists the best-fit parameters for this model, which, as we discuss in §4, we believe provides the best description of the *Chandra* spectrum of RT Cru.

In the first-order spectrum, we detect the iron-line complex spanning roughly 6.4 – 7.0 keV. Fig. 2 shows the region around the iron-line complex in the combined MEG and HEG first-order ( $m = \pm 1$ ) spectrum. Because of the large absorption and the resulting low count rate at low energies, we are not sensitive to lines such as OVIII ( $\sim 19$  Å) and Ne X ( $\sim 12$  Å) that have been seen in HETG observations of some other accreting WDs (e.g., Pandel et al. 2005; Mukai et al. 2003). For the Fe lines, we use a simple powerlaw to establish a continuum level and three Gaussian profiles to fit the Fe K $\alpha$ , H-like Fe, and He-like Fe lines, respectively. To avoid the possible introduction of errors from misalignment of the HEG and MEG spectra, we use only the combined HEG first-order ( $m = \pm 1$ ) spectrum for computation of the equivalent widths (EWs). Table 2 lists the line-center energies and EWs. Although we do not have enough counts to use the recombination, intercombination, and forbidden components of the H- or He-like Fe lines as density diagnostics, the observed line strengths and EWs confirm that the source is surrounded by a large amount of neutral material and that the abundances might be slightly sub-solar. The Fe K $\alpha$  EW of 108 eV is consistent with that expected for a source inside a cloud of cold material with the  $N_H$  of  $\sim 10^{23}$  cm $^{-2}$  (Inoue 1985), as we found from the continuum fitting.

#### 3.2. Timing Analysis

Examining time series binned at 508.208 s and 4065.664 s (i.e., 200 and 1600 times the frame time, respectively), we detected significant aperiodic, flickering-type variations on time scales of minutes to hours in the 0.3–4.0 keV emission. Figure 3 shows the 508-s binned time series (light curves) in the energy ranges 0.3–4.0 keV and 4.0–8.0 keV. The fractional amplitude of the stochas-

tic variations appears to be largest in the 0.3–4.0 keV energy range. In the 508-s binned 0.3–4.0 keV time series, the ratio of measured fractional rms variation,  $s$ , to that expected from Poisson fluctuations alone,  $s_{exp}$ , is 1.96 ( $s = 36.6\%$  and  $s_{exp} = 18.7\%$ ). We detect the 0.3–4.0 keV variability with even greater statistical significance in the 4065-s binned time series; the ratio  $s/s_{exp}$  in this case is 3.35 ( $s = 22.1\%$  and  $s_{exp} = 6.6\%$ ). In the 4.0–8.0 keV energy range, the 508-s binned time series has  $s/s_{exp} = 1.36$  (where  $s = 16.6\%$  and  $s_{exp} = 12.2\%$ ), and the 4065-s binned time series has  $s/s_{exp} = 1.42$  ( $s = 6.1\%$  and  $s_{exp} = 4.3\%$ ).

We do not detect any periodic flux modulations. We are theoretically sensitive to an oscillation with fractional amplitude:

$$A \approx 2 (C_{tot}\alpha)^{-1/2} \left( \ln \left[ \frac{1 - \delta}{1 - (1 - \epsilon)^{1/n_{freq}}} \right] \right)^{1/2} \quad (1)$$

$$= 0.08 \left( \frac{C_{tot}}{9,400} \right)^{-1/2} \left( \frac{\alpha}{0.77} \right)^{-1/2}, \quad (2)$$

where  $C_{tot}$  is the total number of counts in the observation (ignoring the small number of background counts, which have a negligible effect),  $\delta$  and  $\epsilon$  are small numbers related to the chance that a noise power in the power spectrum will exceed the detection threshold (both taken to be 0.05),  $n_{freq}$  is the number of frequencies searched ( $n_{freq} = 1644$ ), and  $\alpha$  has an average value of 0.77 and depends upon the location of the signal frequency in the frequency bin (see, e.g., van der Klis 1989; Sokolowski 1999). We are therefore sensitive to oscillations with fractional amplitudes of  $\sim 8\%$  in regions of the power spectrum dominated by white noise, which in this case consisted of frequencies greater than  $\sim 1.4$  mHz. In this analysis, we binned the time series in 15-s bins (i.e., 6 times the frame time). We were therefore sensitive to oscillations with periods as short as 30 s, and most sensitive to oscillations with periods between 30 s and 12 m.

Consistent with the presence of flickering in the light curves, the power spectrum rises at frequencies below 1.4 mHz. At these low frequencies, the power spectrum has a powerlaw index (i.e., slope on a log-log plot) of about  $-1$ . This “ $1/f$ -noise” at low frequencies reduces our sensitivity to oscillatory signals with periods greater than approximately 12 m. Since we expect the minimum oscillation amplitude to which we are sensitive to increase roughly as the square root of the rising average broadband power as we go to lower frequencies (i.e., longer periods), the oscillation amplitude required for detection increases gradually from  $\gtrsim 8\%$  to  $\gtrsim 15\%$  as we move from periods of 12 m to 1 hr. Taking into account the underlying broadband power, as well as the number of frequency bins searched, we did not detect any statistically significant oscillations in any portion of the power spectrum.

#### 4. DISCUSSION

##### 4.1. Interpretation of the *Chandra* Observations

To estimate the radius of the accreting compact object, we take the unabsorbed 0.3–8.0 keV X-ray luminosity,  $L_X$ , to be either approximately equal to, or a rough lower limit to, the emission from an accretion-disk boundary layer (we justify the assumption that the *Chandra* X-ray emission emanates from a boundary layer in the para-

graphs that follow). Comparing this luminosity with that expected from accretion,  $(1/2)(GM\dot{M}/R) \gtrsim L_X$ , the radius of the accreting compact object is:

$$R \lesssim 3.2 \times 10^8 \text{ cm} \left( \frac{M}{1.3M_\odot} \right) \left( \frac{\dot{M}}{1.8 \times 10^{-9} M_\odot \text{ yr}^{-1}} \right), \quad (3)$$

where  $R$  and  $M$  are the radius and mass of the accretor, respectively, and  $\dot{M}$  is the rate of accretion through the boundary layer. The radius is that of a WD. The *Chandra* X-ray spectrum therefore confirms that the compact object is a WD.

To determine whether the *Chandra*-band X-ray emission is indeed from an accretion-disk boundary layer, we consider the rapid variability. Rapid flickering typically emanates from an accretion region close to a compact object. Our detection of flickering therefore suggests that the X-ray emission detected from RT Cru by *Chandra* is powered by accretion. This accretion could proceed via a wind-fed accretion disk, magnetic accretion columns, or Bondi-Hoyle type direct-impact of the accreting material onto the WD. While the two-component (thermal plasma plus powerlaw) model provides a formally acceptable fit to the data, it is difficult to construct an interpretation of this model that is consistent with the rapid flickering from accretion onto a WD. The isobaric cooling-flow spectral model, on the other hand, 1) provides a good fit to the data, 2) has been successfully applied to both the boundary layer emission from non-magnetic CVs (e.g., Mukai et al. 2003; Pandel et al. 2005) and the accretion columns of magnetic CVs (e.g., Cropper et al. 1998), and 3) provides a natural context for the flickering from accretion.

Most CVs with X-ray emission as hard as that which INTEGRAL and *Swift*/BAT have detected from RT Cru have magnetic fields strong enough to channel the accretion flow into accretion columns ( $B \sim 10^5 - 10^6$  G, where  $B$  is the magnetic field strength at the WD surface). Of the 8 CVs detected at energies greater than  $\sim 50$  keV with *Swift*/BAT, all but SS Cyg are likely magnetic accretors (Barlow et al. 2006). In these systems, the hard X-rays come from hot gas behind the stand-off shock in the accretion column. Magnetic CVs typically have X-ray oscillations with pulsation amplitudes of tens of percent at the WD spin period, which is usually less than an hour (Warner 1995). Since typical symbiotic-star accretion rates are higher than typical CV accretion rates, if the WD in RT Cru was strongly magnetic and in spin equilibrium, the spin period would probably be either comparable to or faster than those in CVs. Given our sensitivity to oscillations with periods less than an hour, we therefore should have detected a spin modulation if RT Cru was magnetic. In fact, the power spectrum has no statistically significant peaks. We conclude that RT Cru is probably not a magnetic accretor. We thus favor the picture in which the X-ray emission from RT Cru detected by *Chandra* is from a cooling flow in an accretion-disk boundary layer.

##### 4.2. Implications

The parameters of the cooling-flow fit to the boundary-layer emission provide the accretion rate as well as information about the WD. From the normalization param-

eter of the cooling-flow model, the accretion rate onto the WD is  $\dot{M} = 1.8 \times 10^{-9} M_{\odot} \text{ yr}^{-1} (d/2 \text{ kpc})^2$  (see Table 1). Since quasi-steady nuclear burning is frequently present on the WD surface, symbiotic stars should have accretion rates that are on average higher than those in CVs. The accretion rate we have found for RT Cru is consistent with this picture. It is also, however, just low enough that we expect the boundary layer to remain optically thin; Narayan & Popham (1993) find that for a  $1 M_{\odot}$  WD, the boundary layer remains optically thin for accretion rates below  $3 \times 10^{-9} M_{\odot} \text{ yr}^{-1}$ .

The parameters of the cooling-flow fit also indicate that the WD radius is small, suggesting that the WD could be quite massive. Taken at face value, the radius constraint would imply that the WD mass is at least  $1.3 M_{\odot}$ . The high upper cooling-flow temperature,  $kT_{max} \geq 55 \text{ keV}$  (see Table 1), supports the conclusion that the accretor is a massive WD. The relationship between  $kT_{max}$  and WD mass is due to the fact that the Kepler velocity ( $v_K^2 = GM/R$ ) is greater in the deep potential well of a more massive WD. Since the boundary-layer material is shock heated, and the initial post-shock temperature ( $T_{max}$ ) is proportional to velocity squared,  $T_{max}$  increases with WD mass. Alternatively, if we equate the amount of energy available per particle,  $(1/2)\mu m_p v_K^2$ , where  $\mu$  is the mean molecular weight and  $m_p$  is the mass of a proton, with the energy released per particle in an isobaric cooling flow,  $(5/2)kT_{max}$  (Pandel et al. 2005), we see that  $kT_{max} \propto v_K^2 \propto GM/R$ . Although the determination of  $kT_{max}$  from X-ray emission below 8 keV is highly uncertain, we can still ask what such a high  $kT_{max}$  would imply if it is confirmed by an instrument with greater high-energy sensitivity (such as SUZAKU). For their sample of 9 non-magnetic CVs, Pandel et al. (2005) found the upper cooling-flow temperature was roughly consistent with the expected  $kT_{max} = (3/5)kT_{vir}$ , where  $T_{vir}$  is the virial temperature (defined by  $(3/2)kT_{vir} = (1/2)\mu m_p v_K^2$ ). Using the WD mass-radius relationship of Hansen & Kawaler (1994), a maximum cooling-flow temperature of  $kT_{max} > 55 \text{ keV}$  implies  $M \gtrsim 1.3 M_{\odot}$ .

The high absorbing columns for both the partial-covering and fully covering absorber, as well as the covering factor of  $>0.7$  for the partial-covering absorber (see Table 1), indicate that the X-ray source is highly obscured at this epoch. Since the X-ray emission region is small, the absorber that only partially covers the X-ray source must also be small. A possible source of this partially covering absorber is an accretion structure such as an accretion disk seen almost edge-on (as in OY Car; Pandel et al. 2005). We assume that the fully covering component of the absorption comprises both interstellar absorption ( $1.1 \times 10^{22} \text{ cm}^{-2}$  from NASA/IPAC IRSA) and intrinsic absorption. The column density of this absorber is probably high because the WD orbits within the strong, dense stellar wind from the red giant. RT Cru has an orbital period of  $\sim 450 \text{ d}$  (J. Miłojewska, *private communication*), and therefore a binary separation on the order of an AU. This separation puts the WD well within the dense region of the red-giant wind. Month-time-scale variations in the absorption (not correlated with the orbital period) have been detected by *Swift* (Kennea et al. 2007), suggesting that either the red-giant

wind is clumpy, that the mass loss rate in the wind of the red giant is variable, or the accretion structure or structures partially blocking the WD boundary layer must be unstable.

#### 4.3. The Nature of RT Cru

As shown by the INTEGRAL detection in 2003-2004 (Chernyakova et al. 2005), RT Cru can at times produce X-ray emission out to greater than 60 keV. From the broad-band flux densities reported by Chernyakova et al. (2005), the hard X-ray spectrum in 2003 - 2004 appears consistent with a powerlaw with photon index  $\Gamma = 2.7$  (energy index  $\alpha = 1.7$ ), and the 16-100 keV luminosity at that time was approximately  $10 L_{\odot} (d/2 \text{ kpc})^2$ . By 2005, however, the 16-100 keV luminosity had dropped, and the hard X-ray spectrum was closer to thermal (Kennea et al. 2007). To better appreciate the properties of the unusual accreting WD in RT Cru, we briefly explore the possible sources of the powerlaw hard X-ray emission observed by INTEGRAL in 2003-2004. In particular, we consider direct synchrotron emission, inverse-Compton (IC) scattering from a thermal distribution of electrons, and IC scattering from a non-thermal distribution of electrons. IC scattering from a non-thermal distribution of electrons turns out to be the most likely option.

One way to generate a powerlaw energy spectrum is with synchrotron emission from a powerlaw distribution of relativistic electrons moving in a magnetic field. Most of the synchrotron emission from an electron with Lorentz factor  $\gamma$  is emitted at a frequency  $\nu_{sync} = (0.3/2\pi)(3 \sin \alpha/2)\gamma_{sync}^2(qB/m_e c)$ , where  $\alpha$  is the pitch angle,  $q$  is the electron charge,  $B$  is the magnetic field strength,  $m_e$  is the electron mass, and  $c$  is the speed of light (Rybicki & Lightman 1979). Since we did not detect X-ray pulsations from RT Cru, the magnetic field at the surface of the WD is probably not strong enough to disrupt the accretion flow, and therefore less than  $\sim 10^4 \text{ G}$ . Thus, even near the surface of the WD, Lorentz factors  $\gamma_{sync}$  of a few times  $10^4$  to  $10^5$  would be needed to produce significant direct synchrotron emission at 60 keV. We can estimate the maximum Lorentz factor to which electrons will be accelerated by setting the diffusive shock acceleration time scale equal to the synchrotron cooling time scale. Following the approach of Markoff et al. (2001), we equate the synchrotron loss rate to a conservative acceleration rate (see Jokipii 1987) to find a maximum Lorentz factor to which electrons can be accelerated of  $\gamma_{max} \approx 2700(B/10^4 \text{ G})^{-1/2}(\xi/100)^{-1/2}$ , where  $\xi$  is the ratio of the diffusive scattering mean free path to the gyroradius. Thus  $\gamma_{max}$  is one to two orders of magnitude below  $\gamma_{sync}$ . Moreover, whereas significant power from a distribution of synchrotron-emitting relativistic electrons would also be expected at energies below 15 keV, the 16-100 keV X-ray luminosity of  $\sim 10 L_{\odot}$  during 2003 and 2004 is already close to the total energy budget available from accretion. Finally, to generate the X-ray spectral index observed by INTEGRAL from direct synchrotron emission, one would need a distribution of electrons that is much steeper than expected from standard theories of particle acceleration in shocks (Ellison et al. 1990). It is therefore unlikely that the hard X-ray emission from RT Cru was due to direct syn-

chrotron emission.

As an aside, we note that the production of significant synchrotron emission at radio wavelengths would not require such high Lorentz factors. The ratio of synchrotron power to IC power from an electron is equal to the ratio of the energy density in the magnetic field to energy density in photons (Rybicki & Lightman 1979). Examining this ratio as a function of distance from the WD, we expect a similar amount of power from direct synchrotron and IC scattering near the surface of the WD, where the B field could be strong ( $B \sim 10^4$  G). We therefore suggest that the next time RT Cru is in a powerlaw hard X-ray state like the one detected by INTEGRAL in 2003-2004, radio observations be performed to look for radio synchrotron emission.

Hard X-rays can be produced with much lower Lorentz factors through IC scattering. For photons scattering off of a thermal distribution of electrons, Reynolds & Nowak (2003) give a relation between the observed photon index  $\Gamma$  and the Compton  $y$  parameter, which is related to the factor by which the average photon energy increases. A steep photon index of  $\Gamma > 2$  indicates a  $y$  parameter less than 1, in which case there is no significant up-scattering. Therefore, since RT Cru had a steep photon index of  $\Gamma \approx 2.7$ , scattering off of a thermal distribution of electrons could not have been responsible for the powerlaw hard X-ray emission. Non-thermal, relativistic electrons must have been involved in producing the powerlaw spectrum observed by INTEGRAL. RT Cru thus contains a white dwarf that can accelerate electrons to relativistic speeds. Three other systems that contain WDs that also generate relativistic electrons are CH Cyg, RS Oph, and possibly R Aqr, all of which have jets (Rupen et al. 2007; O'Brien et al. 2006; Crocker et al. 2001; Nichols et al. 2007).

Assuming now that the powerlaw hard X-ray spectrum was due to IC scattering from a powerlaw distribution of relativistic electrons, we can estimate the location of the scattering electrons. Since the strength of a dipole  $B$  field falls like  $1/r^3$ , whereas the energy density in the photon field only falls like  $1/r^2$ , IC scattering will dominate as one moves farther from the WD. If we ask how far away from the radiation source the IC region should be to give us an IC cooling time on the order of a year (the approximate duration of the powerlaw hard X-ray state), we find that it should be a few tenths of an AU away. Given the orbital period for this systems, that could put the IC emission region either between the WD and the red giant, as in a colliding-winds region, above the WD disk in a corona, or at the base of a jet. A model consisting of IC scattering off of relativistic electrons in a corona or at the base of a jet reproduces the observed hard X-ray emission well in X-ray binaries (Markoff et al. 2005). The steep powerlaw index, which is similar to that seen in the steep powerlaw state in microquasars, could be due

to a low scattering optical depth (Rybicki & Lightman 1979).

## 5. CONCLUSIONS

We have observed the first symbiotic star with X-ray emission out to greater than 60 keV with the HETG on *Chandra*. The stochastic variability and cooling-flow type spectrum suggest that RT Cru is powered by accretion onto a WD through a disk with an optically thin boundary layer. The accretion rate is near the top of the range for which the boundary layer can remain optically thin. The high initial temperature of the cooling flow, and the high luminosity given the accretion rate from the spectral fit suggest that the WD in RT Cru could be quite massive. More generally speaking, it would be difficult to get such hard X-ray emission from accretion onto a low-mass WD with a shallow potential well and low Kepler velocity. Given the nature of the powerlaw hard X-ray emission previously observed by INTEGRAL, it therefore appears that the accreting, non-magnetic WD in RT Cru is able to generate a non-thermal, powerlaw distribution of electrons and very hard X-ray emission through IC scattering. Three other systems in which WDs can accelerate electrons to relativistic speeds (RS Oph, CH Cyg, and possibly R Aqr; Rupen et al. 2007; O'Brien et al. 2006; Crocker et al. 2001; Nichols et al. 2007) all have jets. Radio observations of RT Cru during the next powerlaw hard X-ray state like that observed by INTEGRAL in 2003 and 2004 could play an important role in diagnosing this system, and determining the extent to which some symbiotic stars might constitute the nanoquasar analog to microquasars (Zamanov & Marziani 2002).

We thank the referee, Marina Orio, for comments and suggestions which improved the final quality of this article. We also thank K. Mukai, F. Paerels, T. Maccarone, and A. J. Bird for useful discussions, R. Lopes de Oliveira and D. Huenemoerder for help with the data analysis, and S. Markoff for comments on the manuscript. G.J.M. Luna acknowledges support from CNPq (process 0141805/2003-0) and FAPESP (process 02/08816-5). J.L.S. is supported by an NSF Astronomy and Astrophysics Postdoctoral Fellowship under award AST-0302055. Support for this work was provided by the National Aeronautics and Space Administration through Chandra Award Numbers DD5-6034X and NNX06AII6G issued by the Chandra X-ray Observatory Center, which is operated by the Smithsonian Astrophysical Observatory for and on behalf of the National Aeronautics Space Administration under contract NAS8-03060. We acknowledge with thanks the variable star observations from the AAVSO International Database contributed by observers worldwide and used in this research.

## REFERENCES

- Arnaud K. A., 1996, *Astronomical Data Analysis Software and Systems V*, eds. Jacoby G. and Barnes J., p17, ASP Conf. Series volume 101.
- Anders E. & Grevesse N., 1989, *Geochimica et Cosmochimica Acta* 53, 197
- Barlow, E. J., Knigge, C., Bird, A. J., J Dean, A., Clark, D. J., Hill, A. B., Molina, M., & Sguera, V. 2006, *MNRAS*, 372, 224
- Bird, A. J., et al. 2007, *ApJS*, 170, 175
- Belczyński, K., Mikolajewska, J., Munari, U., Ivison, R. J., Friedjung, M., 2000, *A&AS*, 146,407
- Canizares, C. et al. 2005, 117, 1144
- Chakrabarty, D., & Roche, P. 1997, *ApJ*, 489, 254
- Chernyakova M., Courvoisier T. J., Rodriguez J., Lutovinov A., 2005, *The Astronomer's Telegram*, 519,1

- Cieslinski D., Elizalde F., Steiner J. E., 1994, *A&A*, 106, 243
- Crocker M. M., Davis R. J., Eyres S. P. S., Bode M. F., Taylor A. R., Skopal A., Kenny H. T., 2001, *MNRAS*, 326, 781
- Crocker M. M., Davis R. J., Spencer R. E., Eyres S. P. S., Bode M. F., Skopal A., 2002, *MNRAS*, 335, 1100
- Cropper M., Ramsay G., Wu K., 1998, *MNRAS*, 292, 222
- Davidson, A., Malina, R., & Bowyer, A. 1977, *ApJ*, 211, 866
- Done, C., & Magdziarz, P. 1998, *MNRAS*, 298, 737
- Ellison, D. C., Reynolds, S. P., & Jones, F. C. 1990, *ApJ*, 360, 702
- Galloway, D. K., Sokolowski, J. L., & Kenyon, S. 2002, *ApJ*, 580, 1065
- Houck, J. C., High Resolution X-ray Spectroscopy with XMM-Newton and Chandra, Proceedings of the international workshop held at the Mullard Space Science Laboratory of University College London, Holmbury St Mary, Dorking, Surrey, UK, October 24 - 25, 2002, Ed. Branduardi-Raymont, G., published electronically and stored on CD., meeting abstract
- Hachisu, I., & Kato, M. 2001, *ApJ*, 558, 323
- Hansen, C. J., & Kawaler, S. D. 1994, *Stellar Interiors. Physical Principles, Structure, and Evolution*, XIII, Springer-Verlag Berlin Heidelberg New York
- Harris D. E., Mossman A. E., Walker R. C., 2004, *ApJ*, 615, 161
- Inoue H., 1985, *Sp. Sci. Rev.*, 40, 317
- Jablonski, F. J., Pereira, M. G., Braga, J., & Gneiding, C. D. 1997, *ApJ*, 482, L171
- Jokipii, J. R. 1987, *ApJ*, 313, 842
- Jordan S., Müerset U. & Warner K., 1994, *A&A*, 283, 475
- Karovska, M., Carilli, C. L., Mattei, J. A., 1998, *JAVSO*, 26, 97
- Karovska M., Schlegel E., Hack W., Raymond J., Wood B. E., 2005, *ApJ*, 623, 137
- Kenyon, S. J., *The symbiotic stars*, 1986, Cambridge University Press
- Kennea, J., Mukai, K., et al. 2007 in prep.
- Luna, G. J. M., Sokolowski J. L., Mukai K., Costa, R. D. D., in prep.
- Livio M., 1997, in: *Accretion Phenomena and Related Outflows*, IAU Colloquium 163, ASP Conf. Series, Vol. 121, D. T. Wickramasinghe, L. Ferrario & G. V. Bicknell, eds., p. 845
- Makishima, K. 1986, in *The Physics of accretion onto Compact Objects*, eds. K. O. Mason, M. G. Watson & N. E. White, Springer Verlag Berlin, p249
- Markoff, S., Falcke, H., & Fender, R. 2001, *A&A*, 372, L25
- Markoff, S., Nowak, M. A., & Wilms, J. 2005, *ApJ*, 635, 1203
- Masetti, N., et al. 2002, *A&A*, 382, 104
- Masetti, N., Bassani L., Bird A. J., Bazzano A., 2005, *The Astronomer's Telegram*, 528
- Masetti N, Bassani L., Dean A. J., Ubertini P., Walter R., 2006, *The Astronomer's Telegram*, 715
- Masetti, N., et al. 2007, *A&A*, 464, 277
- Masetti, N., et al. 2007, *A&A*, 470, 331
- Mushotzky R. F. & Szymkowiak A. E., 1988, *Cooling Flows in Clusters and Galaxies* ed. A. C. Fabian, p. 53
- Mukai K., Kinkhabwala A., Peterson J. R., Kahn S. M., Paerels F., 2003, *ApJ*, 586, 77
- Mukai K., Ishida M., Kilbourne C., Mori H., Terada Y., Chan K., Soong Y., 2007, *PASJ*, 59, 177
- Müerset U., Wolff B., Jordan S., 1997, *A&A*, 319, 201
- Narayan, R., & Popham, R. 1993, *Nature*, 362, 820
- Nichols, J. S., DePasquale, J., Kellogg, E., Anderson, C. S., Sokolowski, J., & Pedelty, J. 2007, *ApJ*, 660, 651
- O'Brien, T. J., et al. 2006, *Nature*, 442, 279
- Orio M., Zezas A., Munari U., Siviero A., Tepedelenioglu E., 2007, *ApJ*, 661, 1105
- Pandel D., Córdoba F. A., Mason K. O., Priedhorsky W. C., 2005, *ApJ*, 626, 396
- Reynolds, C. S., & Nowak, M. A. 2003, *Phys. Rep.*, 377, 389
- Rupen, M. J., Mioduszewski, A. J., & Sokolowski, J. L. 2007, submitted to *ApJ*
- Rybicki, G. B., & Lightman, A. P. 1979, New York, Wiley-Interscience, 1979, p. 179
- Sokolowski, J. L. 1999, Ph.D. Thesis, U.C. Berkeley
- Sokolowski, J. L. 2003, *Astronomical Society of the Pacific Conference Series*, 303, 202
- Sokolowski J. L., Bildsten L., Ho W. C. G. 2001, *MNRAS*, 326, 553
- Sokolowski J., Kenyon S. J., 2003, *ApJ*, 584, 1021
- Sokolowski J. L., Kenyon S. J., Espey B. R., Keyes C. D., McCandliss S. R., Kong A. K. H., Aufdenberg J. P., Filippenko A. V., Li W., Brocksopp C., et al., 2006, *ApJ*, 636, 1002
- Taylor A. R., Seaquist E. R., Mattei J. A., 1986, *Nature*, 319, 38
- Tueller J., Gehrels N., Mushotzky R. F., Markwardt C. B., Kennea J. A., Burrows D. N., Mukai K., Sokolowski J., 2005, *The Astronomer's Telegram*, 591
- Tueller J., Barthelmy S., Burrows D., Falcone A., Gehrels N., Grupe D., Kennea J., Markwardt C. B., Mushotzky R. F., Skinner G. K., 2005, *The Astronomer's Telegram*, 669
- van Belle, G. T., et al. 1999, *AJ*, 117, 521
- van der Klis, M. 1989, in *Timing Neutron Stars* (Kluwer Academic Publishers), Ögelman, H., & van den Heuval, E. P. J. eds., p27
- Warner, B. 1995, *Cataclysmic Variable Stars* (Cambridge University Press: Cambridge)
- Zamanov, R., & Marziani, P. 2002, *ApJ*, 571, L77

TABLE 1  
COOLING-FLOW MODEL PARAMETERS.

Parameter	Value (Min, Max) <sup>a</sup>
$\dot{M}^b$ ( $10^{-9} M_{\odot} \text{ yr}^{-1}$ )	1.8 (1.6, 2.0)
$kT_{max}$ (keV)	80 (56, ...)
$n_H$ : Full covering ( $10^{22} \text{ cm}^{-2}$ )	8.2 (7.7, 8.8)
$n_H$ : Partial covering ( $10^{22} \text{ cm}^{-2}$ )	65 (52, 78)
Covering Fraction	0.74 (0.69, 0.79)
Abundance (w.r.t. Solar <sup>c</sup> )	0.30 (0.02, 0.45)
$F_X^d$ ( $10^{-12} \text{ erg cm}^{-2} \text{ s}^{-1}$ )	9.1 (7.5, 10.2)
$L_X^d$ ( $10^{34} \text{ erg s}^{-1}$ )	3.1 (2.4, 3.9)

NOTE. — The model consists of optically thin thermal emission from an isobaric cooling flow with absorbers that both fully cover and partially cover the source, plus a Gaussian line.

<sup>a</sup> 90% confidence upper and lower limits.

<sup>b</sup> Accretion rate onto the compact object.

<sup>c</sup> Using solar abundance of Anders & Grevesse (1989).

<sup>d</sup>  $F_X$  is the absorbed 0.3–8.0 keV flux, and  $L_X$  is the unabsorbed 0.3 – 8.0 keV luminosity ( $d = 2$  kpc).



TABLE 2  
IRON LINES.

	Fe XXV	Fe XXVI	Fe $K\alpha$
Line center (keV) <sup>a</sup> :	6.946 <sup>6.959</sup> <sub>6.933</sub>	6.693 <sup>6.706</sup> <sub>6.677</sub>	6.379 <sup>6.399</sup> <sub>6.358</sub>
EW <sup>b</sup> (eV):	72	60	108

<sup>a</sup> Super- and subscripts represent 90% confidence upper and lower limits, respectively.

<sup>b</sup> Gaussian-fit equivalent widths. EW uncertainties are on the order of 10–15%.

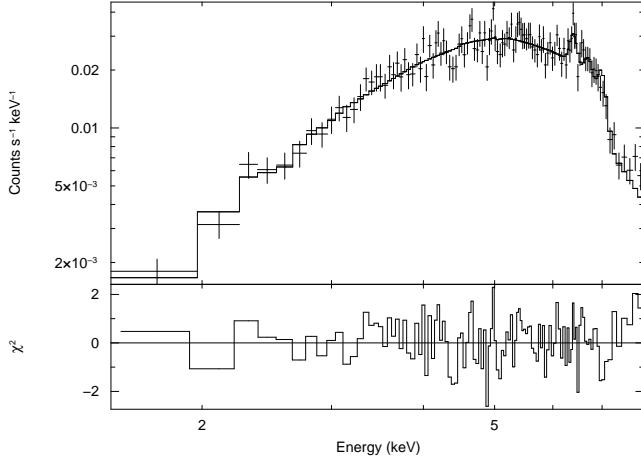


FIG. 1.— Undispersed (zeroth order) spectrum. The top panel shows the spectrum with the absorbed, isobaric cooling-flow model over-plotted. The bottom panel shows residuals with respect to this model (in units of  $\chi^2$ , where  $\chi^2$  is shorthand for the difference between the data and the model, squared, divided by the variance, with the sign of the difference between the data and the model).

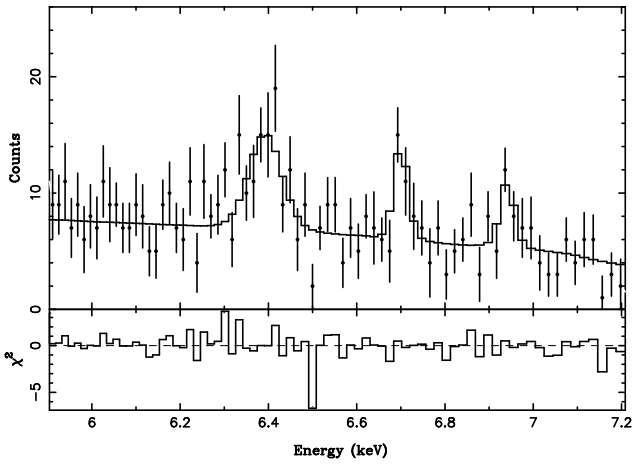


FIG. 2.— The iron-line complex from the combined HEG and MEG first-order ( $m = \pm 1$ ) spectrum. The best fit model of a powerlaw plus three Gaussian emission lines is over-plotted. The bottom panel shows the residuals, in the same units as Fig. 1.

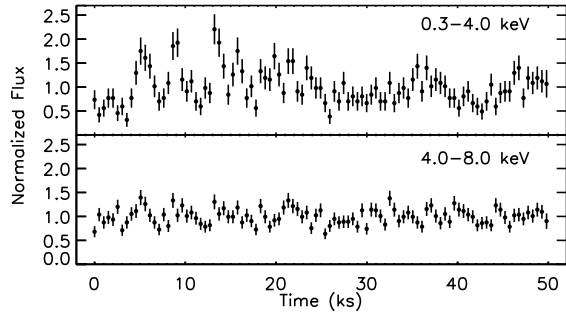


FIG. 3.— *Chandra* light curves for RT Cru, with a bin size of 508.28 s. The light curves include the undispersed light as well as the counts from the HEG and MEG  $m = \pm 1$  orders. The top and bottom panels show the flux as a function of time in the energy ranges 0.3–4.0 keV and 4.0–8.0 keV, respectively. The 0.3–4.0 keV emission is clearly variable on time scales of minutes to hours.